Renewable Energy 83 (2015) 1110–1118

Contents lists available at ScienceDirect

Renewable Energy

journal homepage: www.elsevier.com/locate/renene

Electrical production of a small size Concentrated Solar Power plant with compound parabolic collectors

M. Antonelli*, A. Baccioli, M. Francesconi, U. Desideri, L. Martorano

University of Pisa, Largo Lucio Lazzarino, Pisa 56125, Italy

ARTICLE INFO

Article history:
Received 1 March 2014
Accepted 12 March 2015
Available online 10 June 2015

Keywords:
Solar energy
Distributed generation
Organic Rankine Cycle
Compound parabolic collectors
AMESim
Lumped parameters model

ABSTRACT

The use of the solar energy for electricity or useful heat generation has been extensively investigated as an alternative to fossil fired energy conversion. Particularly in the last decade, many studies have been carried out on Concentrated Solar Power (CSP) which was developed worldwide with Spain acting as the leading country in this field. Concentrating solar energy requires complex mirror systems which continuously move to track the sun. In comparison with flat mirrors, Parabolic Through Collectors (PTCs) have allowed to reduce costs, but they still remain quite an expensive solution. Instead, compound parabolic collectors (CPCs) are able to collect a higher fraction of both the direct and the diffuse radiation, although they have a lower efficiency at high temperature. Moreover, at least within certain limits, they do not require a tracking system. Their employment is therefore suited for the collection of medium temperature heat (up to 200 °C) and is useful for the reduction of the installation cost of Concentrated Solar Power (CSP) heating/cooling and energy generation systems. Small size plants (10–50 kW) were studied in this paper since they are more likely to be realized due to their smaller initial investment cost and to the capability of being installed on the roof of existing buildings. While the Organic Rankine Cycle (ORC) solution is well established to be the optimal for small size, distributed generation plants, the technology of the expansion device is still to be defined for the investigated installed power range. Accordingly to previous studies, an expansion device based on the Wankel mechanism was employed.

Based on these considerations and prior to more detailed analyses, a study of the annual energy production of a small scale ORC power plant using CPCs as a heat source and a volumetric machine as an expansion device was carried out. The influence of the thermodynamic cycle parameters, the working fluid, the concentration and the tilt angle of the collectors on the electrical energy production were taken into account. The thermal module power output, the expansion device isentropic efficiency and the overall efficiency were evaluated by means of a numerical model developed within the simulation tool AMESim v.12.0.

The aim of this work is to provide a contribution in the assessment of the optimal configuration of such kind of plants in terms of collectors concentration and tilt angle on one hand, and thermodynamic parameter of the thermal module on the other. The annual electricity production was used as a criterion of comparison among the various parameters combinations. The number of operating hours per year was also taken into account for the sake of ensuring a regular production of energy. A selection of commercial solar tubes for the realization of the solar field was carried out and the optimal configuration for both the solar field and the thermal module was found. The results of this study are encouraging and constitute the basis for the development of future analyses.

1. Introduction

The attractiveness of the Organic Rankine Cycles (ORCs) mainly resides in that they are able to use low temperature heat sources while operating at relatively high efficiencies, thus enabling the construction of low and medium scale power plants that may be suited to a large variety of applications. Most of these advantages

* Corresponding author.
E-mail address: marco.antonelli@ing.unipi.it (M. Antonelli).

http://dx.doi.org/10.1016/j.renene.2015.03.033
0960-1481/

Nomenclature

a	solar tube thermal loss coefficient
A	area (m^2)
C	concentration
D	direct radiation (kW m^{-2})
I	incident solar radiation (kW)
E	energy amount (kJ)
$\dot{E}$	energy flux (kW)
h	enthalpy (kJ kg^{-1})
H	diffuse radiation (kW m^{-2})
K	proportionality constant
N	number of reflections
$\dot{Q}$	heat flux (kW)
r	radius (m)
R	factor of inclination
T	temperature (K)
U	convective heat transfer (kW m^{-2})
V	displacement (cm^3)
$\dot{W}$	mechanical power (kW)
Z	number of hours

Subscripts

a	ambient
ab	aerocondenser blower
ac	acceptance
ap	approach point
av	average
aux	auxiliaries
c	collector
cd	condensation
cg	cover glass
con	convective
d	daily
df	diffuse
di	direct
ed	expansion device
hf	heat transfer fluid
in	incoming
is	isentropic
l	lost
max	maximum
min	minimum
op	optical
out	outgoing
p	pump
pp	pinch point
r	receiver
ref	reflected
rad	radiative
rem	removal
s	solar
tc	thermal cycle
th	thermal
u	useful
wf	working fluid

Greek

α	sun elevation
β	collectors tilt angle (°)
ε	emissivity
η	efficiency
φ	reflection efficiency
Φ	heat removal factor
γ	collectors azimuthal angle (°)
ρ	radial coordinate (m)
σ	Stefan–Boltzmann constant (kW m^{-2} K^{-4})
θ	angular coordinate (°)

may also fit for solar applications, especially for small-size power plants, in combination with low/medium temperature solar collectors [1–3], where the integration with other resources is always an interesting option (with biomass or geothermal energy for example [4]).

The nature of the working fluid has also been the object of several studies: in the first research works [5,6] high Ozone Depleting Potential (ODP) refrigerants such as R11 or R13 were used. In more recent studies other newly developed refrigerants were used, such as R245fa [7]. The optimization of the fluid selection for different cycle architectures and collectors' temperatures was treated in more recent studies [8–13]. However, no single fluid has been identified as optimal for the ORC, due to the strong interdependence between the working fluid features, the operating conditions and the cycle architecture. Most of the above mentioned studies show that the ORC efficiency is significantly improved by inclusion of a recuperator, of cascaded cycles, or of reheating [9,14,15].

At present, only one commercial solar ORC power plant is reported in the technical literature: the 1 MWe Saguaro Solar ORC plant in Arizona, which uses n-pentane as working fluid and shows an overall efficiency of 12.1%, with a collector efficiency of 59% [16]. The relatively high efficiency of this plant is due to the employment of high concentration tracking parabolic trough collectors.

Lower efficiencies were in facts obtained with stationary collectors. Some authors [7] reported a 3.2% overall efficiency in a 1.6 kWe solar ORC with flat-plate collectors and 4.2% with evacuated tube collectors. A similar efficiency (lower than 4%) was obtained in a 2 kWe low-temperature solar ORC with R134a as working fluid and evacuated tube collectors [17]. In both those experiences, however, the collectors were used without any prior optimization process concerning concentration, tilt angle and collectors alignment. The collectors were aligned in the north–south direction and the originally built-in concentrator was used. For the sake of comparison of the previously mentioned solutions with those with a tracking system, a 7.7% efficiency was reported in a 9 kWe ORC employing a linear Fresnel Collector (collector efficiency of 57%).

Although solar ORCs feature lower efficiencies than photovoltaic (PV) systems, the presence of a thermal storage and even the thermal inertia itself of these plants provide a more stable electrical production, which make their power generation more predictable and easy to dispatch than PV systems. In addition, this technology does not require the employment of advanced or rare materials such as pure silicon. Finally, the use of commonly available and reusable or recyclable materials (steel, plastics, aluminum, copper, etc.) makes the end-life disposal of the plants easier than for PV panels.

Focusing the attention on mini and micro (up to 50 kW) solar applications, the absence of a tracking system and the use of compact design collectors are useful for the reduction of the installation and maintenance costs. In fact, if a maximum cycle temperature of 200 °C is considered, Compound Parabolic Collectors (CPCs) can be used since they do not require a tracking system

and they allow a moderate concentration. These concentrators have been studied for many years, both analytically and practically [18–24] as well as solar ORCs, which reported overall efficiencies varying between 2.5% and 7% [5,25,26].

A study on the off-design performances of a solar ORC was recently presented [27]; the authors discussed on the influence of the various plant parameters on the base of a numerical model which simulated the system over a day (21st june). The plant size was greater than the one taken as a reference within this study and a turbine was chosen by the authors as the expansion device. A single tilt angle and concentration were employed within this study. The concentration was 6.5 and consequently a tracking system was necessary.

The aim of this work is to fill the gap observed in the related literature about the analysis of the optimal combination of the operating parameters of both the solar field (concentration, collectors tilt angle) and the thermal module (thermodynamic parameters, plant configuration). The preliminary study presented about the feasibility of such a system [28] was further extended in the present work through the investigation of the thermal cycle optimal layout, the characterization of collectors built on the basis of commercially available components and a more detailed analysis of the solar field performance.

The optimal solution, to which type of expander is most suited, has not been found yet: some studies proposed the use of vane expanders [5,6], others proposed a rolling piston expander [7] or a machine derived from a Scroll compressor [29]. In the present work the authors propose to use a specifically designed unit, based on the Wankel capsulism, which was described in a previous publication [30–33] where they showed that such device is an effective solution in the 10–50 kW size range. Such an expander, moreover, is more compact than reciprocating devices and is able to rotate at higher speeds with lower vibrations.

This first analysis was carried out at steady state, whereas a study of transient operation is currently in progress and will be the subject of a future paper.

2. Method

A typical layout for small-scale solar systems was taken as a reference (Fig. 1) in which the solar field and the thermal module were connected via a heat transfer fluid circulation (water in this case). Air-cooled condensers with induced-draft fans were considered.

The thermal module included the preheating section, the evaporator, the eventual superheater, the expansion device, the recuperator and the condenser. Its annual electricity production was calculated by means of a numerical model which is described hereinafter. The transient behavior of the solar source was not taken into account here and an average insolation was employed.

Since steady state conditions were investigated, the storage tank, which is usually employed in solar systems, was not modeled. The cogeneration was not taken into account as well since the aim of this study was evaluating the optimal conditions for the electricity generation.

Under the hypothesis of steady state, averaged operating conditions, the annual electricity production was calculated as:

$$E_{an} = \sum_{i=1}^{12} \overline{I_i \cdot Z_i \cdot \eta_{s,i} \cdot \eta_{th,i}} \tag{1}$$

In order to separate the effects of variation of the solar field and the thermal module parameters, the previous relationship was approximated as

$$E_{an} = \simeq \sum_{i=1}^{12} \bar{I}_i \cdot \overline{Z}_i \cdot \overline{\eta}_{s,i} \cdot \overline{\eta}_{th,i} \tag{2}$$

in which $\bar{I}_i$ denotes the solar radiation averaged over the generic i-th month, Z_i is the number of operating days during the i-th month, $\overline{\eta_{si}}$ the solar field average efficiency and $\overline{\eta}_{th,i}$ the thermal cycle average efficiency. For the sake of brevity, in the following lines the superscripts denoting the operation of averaging will be omitted.

2.1. Solar intensity and operating hours

Since the investigated temperature range exceeded 100 °C, based on literature [23] the axis of the absorbers was aligned in east-west direction, differently from other papers found in literature [7,17]. The arrangement used in the present work enabled the use of various concentrations reflectors.

The solar intensity on the collector was calculated at the latitude of the Central Italy (43°) through the model of Liu and Jordan [34] which takes into account the distribution of direct, diffuse and reflected solar radiation:

$$I = R_{di} \cdot D + R_{df} \cdot H + R_{ref} \cdot (D + H) \tag{3}$$

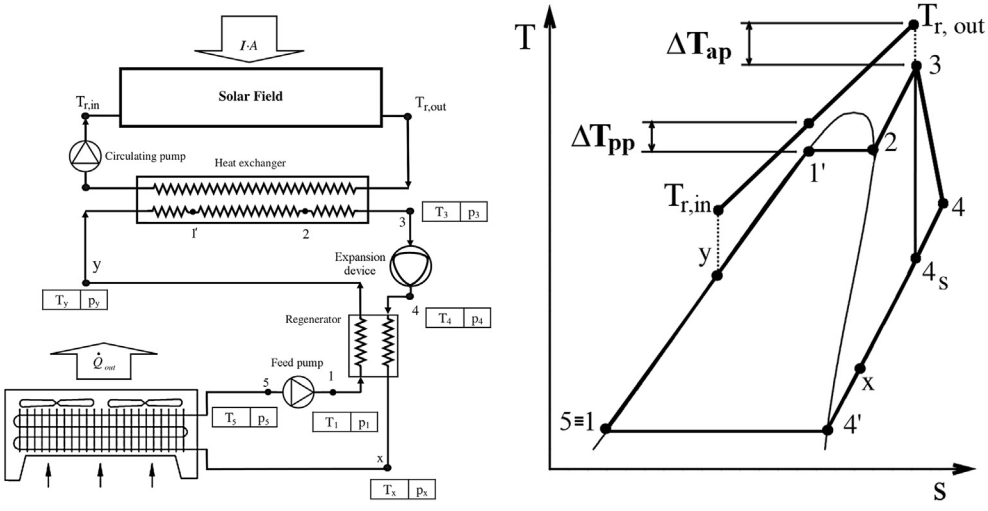

Fig. 1. Schematical plant layout (left) and thermal cycle on the $T - s$ thermodynamic plane (right).

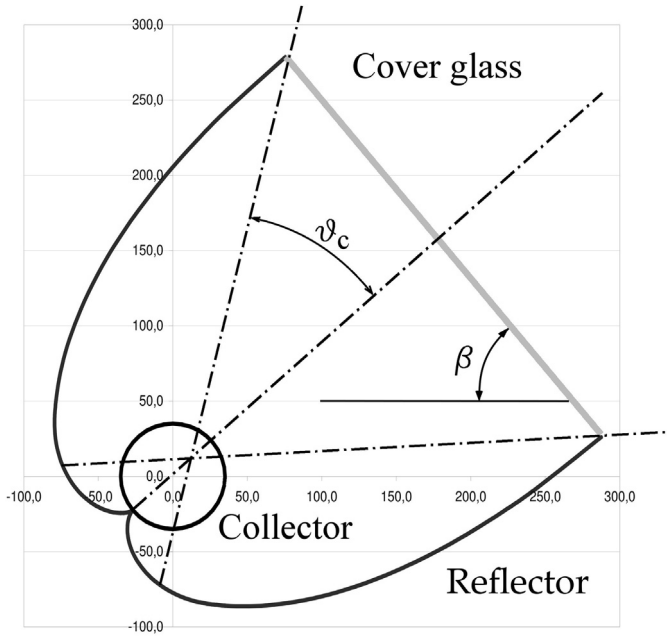

Fig. 2. Schematical view of the section of a Compound Parabolic Collector with $C = 1.5$.

The average number of operating hours per month was calculated by considering the sunrise and the sunset time relative to a surface tilted by β (Fig. 2) with respect to the horizontal and oriented toward the south. The operating hours were furthermore limited by the angle of the collectors.

In order to collect the solar radiation at noon, for each value of θ_{ac}, the maximum collectors tilt angle β_{max} was calculated as:

$$\beta_{max}(C) = \alpha_{max} - (90^{\circ} + \theta_{ac}) \tag{4}$$

At the same time, for each value of β, the minimum angle α_{min} at which the sun radiation was collected by the collectors was calculated as:

$$\alpha_{min} = 90^{\circ} - (\beta + \theta_{ac}) \tag{5}$$

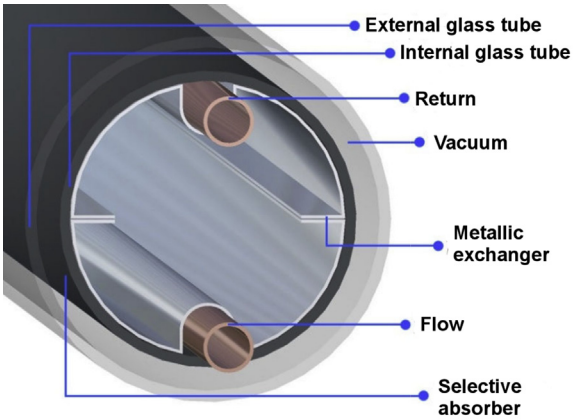

Fig. 3. Representation of an evacuated tube collector with U-pipe.

2.2. Collectors average efficiency

Focusing the attention on small-scale power systems and aiming at the maximum reduction of the installation costs, widely commercially available components such as the U-pipe evacuated tubes were considered (Fig. 3).

The efficiency of the collectors was calculated by taking into account the performances of four types of commercial tubular U-pipe collectors, which are identified in the text by capital letters to avoid any commercialism.

The efficiency of the collectors was calculated through a balance between the incoming and the outgoing energy, namely the solar radiation on one hand, the useful and the lost heat on the other.

$$\dot{E}_{s,in} = \dot{Q}_u + \dot{Q}_l \tag{6}$$

The energy collected by the solar tube $\dot{E}_{s,in}$ was evaluated as the product of the solar radiation by the optical efficiency and the heat removal factor Φ that takes into account the non-constant temperature of the receiver.

$$\dot{E}_{s,in} = \dot{E}_s \cdot \eta_{op} \cdot \Phi = I \cdot C \cdot A_c \cdot \eta_{op} \cdot \Phi \tag{7}$$

The solar field was discretized in a series of collectors where the temperature variation effect was negligible from the point of view of the collector efficiency. The factor Φ consequently had a unit value.

As far as the collector's efficiency is concerned, the technical documentation reports the coefficients η_0 (optical efficiency), a^1 and a^2 (linear and the quadratic terms coefficients, respectively), according to EN 12975 [35] (Table 1). Those coefficients however include the effect of the built-in reflector which usually has a concentration in the range C = 0.6–0.8.

In order to take into account the influence of C on the optical efficiency, a simplified approach, with respect to other models described in literature [36], was employed. The effect of the reflections number N, which is usually provided by well-known datasets for both untruncated and truncated reflectors [1], was accounted here by considering that a generic sunray entering the collector may directly impinge the glass tube or be reflected one time by the reflector and attenuated by the factor φ. In addition, since a U-pipe solar tube was employed instead of a trough collector, the sunrays pass through the glass two times and therefore the relative loss was accounted twice.

The calculated and declared (Table 1) values of the optical efficiency were compared, showing quite a good agreement (Table 2).

This approach also accounted for a slight decrease of the optical efficiency with C, with a certain correspondence with theory (Fig. 4).

The efficiency of the solar collector was evaluated by calculating the convective and the radiating losses to the ambient air:

$$\dot{Q}_l = \dot{Q}_{l,con} + \dot{Q}_{l,rad} = U_l \cdot \frac{A_c}{C}(T_r - T_a) + \sigma\varepsilon_r \cdot \frac{A_c}{C}\left(T_r^4 - T_a^4\right) \tag{8}$$

The tuning of the numerical model coefficients was carried out

Table 1
Main parameters of the solar collectors.

Tube model	η_0 –	a_1 (W/m^2 K)	a_2 (W/m^2 K^2)	C –
A	0.700	1.150	0.011	0.89
B	0.644	0.749	0.005	0.73
C	0.620	0.395	0.020	0.80
D	0.642	0.885	0.001	0.88

Table 2
Comparison between declared and calculated optical efficiency.

Tube model	Declared η_{op}	Calculated η_{op}
A	0.700	0.696
B	0.642	0.645
C	0.620	0.616
D	0.642	0.634

Table 3
Convective heat transfer and emissivity used for calibration.

Tube model	U_l	ε_r
A	0.15	0.195
B	0.26	0.070
C	0.40	0.170
D	0.68	0.020

by varying the convective heat transfer coefficient U_l and the emissivity of the receiver ε_r (Table 3).

The resulting efficiencies of the various collectors were consistent with the ones declared by the companies (Fig. 5) and with other data reported in literature [37–40]. The deviation between the declared and the recalculated efficiency is lower than 1% for all but model C.

All these relationships were finally summarized to allow the model of the solar collector to be included into the model of the whole plant.

As for the inlet and outlet collectors temperature $T_{hf,in}$ and $T_{hf,out}$, their evaluation was carried out by considering (Fig. 2) a fixed value for the temperature difference at the pinch ΔT_{pp} and at the approach point ΔT_{ap} (5 and 10 K, respectively).

2.3. Thermal cycle modeling

The thermal plant efficiency η_{th} was calculated as the ratio of the net power over the heat flux provided by the solar field.

$$\eta_{th} = \frac{\dot{W}_{net}}{\dot{Q}_u} = \frac{\dot{W}_{net}}{\eta_s I} \tag{9}$$

The net power delivered by the plant was evaluated as the difference between the power generated by the expander minus the power employed by the auxiliaries (pump, condenser blowers).

$$\dot{W}_{net} = \dot{W}_{ed} - \dot{W}_p - \dot{W}_{ab} \tag{10}$$

The isentropic efficiency of the pump was assumed to be constant and equal to $\eta_p = 0.7$, from which the power required by the pump was calculated as:

$$\dot{W}_p = \frac{\dot{m}_{wf}\left(p_{vap} - p_{cd}\right)}{\eta_p\, \rho_{wf}} \tag{11}$$

The power required by the aerocondenser blowers was evaluated as proportional to the rejected heat. The proportionality constant K_{ab} was evaluated through a survey of the commercially available components and its value was set at 25 W per thermal kW of rejected thermal power $\dot{Q}_{rj}$ (at the design point, that is to say ΔT between condensing fluid and ambient air equal to 15 °C).

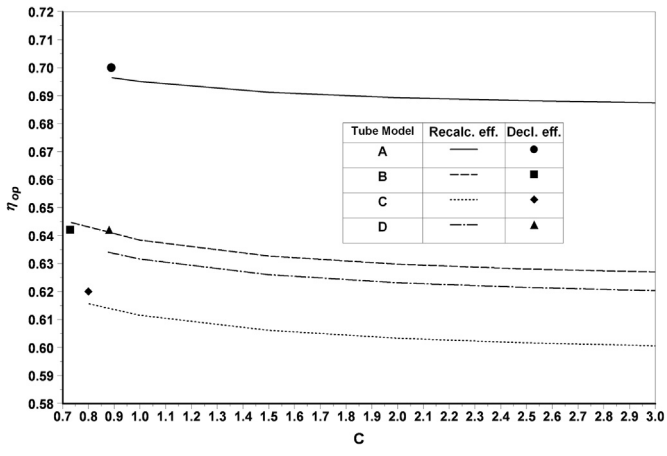

Fig. 4. Optical efficiency as a function of *C*.

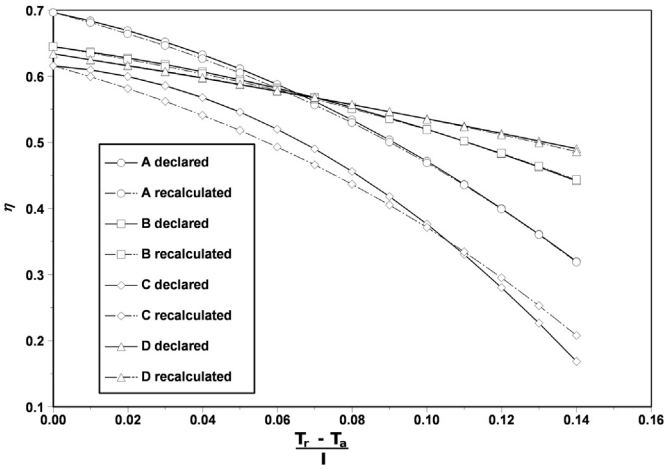

Fig. 5. Collectors efficiency with the original built-in reflector.

$$\dot{W}_{ac} = K_{ab}\,\dot{Q}_{rj} = K_{ab}\left(\dot{Q}_u - \dot{W}_{ed}\right) \tag{12}$$

As for the expansion device, the proposed machine was already analyzed in previously published papers [32,33,41]. Although this machine is a rotary device, the thermodynamic limit cycle is the same of a reciprocating one (Fig. 6).

The numerical analysis was carried out using a numerical model built using the simulation tools AMESim v.12.0, simulating the in-chamber pressure as a function of the crank angle. The numerical model of the Wankel expansion machine was developed in previous works [32], but in this analysis the two-phase fluids library of the code was used to analyze this device operated with organic fluids. The crank angle-volume mathematical relationship of the original "crank angle" model was modified to account the different volume kinematic of the Wankel engine respect to a conventional reciprocating one. The pressure drop across the intake and the exhaust valves was accounted by modeling the valves themselves as variable area orifices. The numerical model of the device was validated by comparing the results with experimental data [41].

Due to the variability of the solar radiation along the year, the expansion device rotating speed was supposed to be variable in order to accomodate the working fluid mass flow rate. This control strategy in facts proved to be effective for this kind of machines, although a certain decrease of η_{is} with the rotating speed was observed [41,42]. Conservatively, η_{is} was supposed to depend on p_2/p_3 and T_2 only and, for every combination of these two parameters, the value assumed at the maximum rotating speed (3000 rpm) was considered.

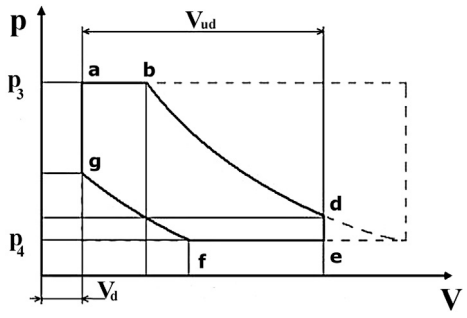

Fig. 6. Expansion device theoretical cycle on the $p - V$ thermodynamic plane.

3. Numerical results and discussion

As pointed out in the literature [43], the choice of the optimal temperature in the receivers is a tradeoff between collector efficiency and ORC efficiency. Increasing the temperature leads to higher thermal losses but also to a higher thermal module conversion efficiency. The optimal conditions may furthermore vary along the year due to the different insolation and ambient temperature. The optimal operating conditions were therefore evaluated respect to the annual electricity production.

3.1. Working fluid and introduction grade

Based on previously published work [28], R-600a was considered as working fluid because, on one hand it provided a somewhat lower delivered power than other fluids (like R-134a and R-152a), on the other it also yielded a better efficiency over a wider temperature range.

Since the performance of a volumetric expansion device is affected by the introduction ratio (Eq. (13)), an appropriate value has to be chosen as a tradeoff between isentropic efficiency and delivered power.

$$\sigma = \frac{V_b - V_a}{V_{ud}} \tag{13}$$

Based on the performed analysis, an introduction ratio of 0.2 enabled the device isentropic efficiency to be equal or above 0.8 over the entire range of the expansion ratio p_3/p_4 (ratio of the upstream over the downstream pressure) included between 3 and 8 (Fig. 7).

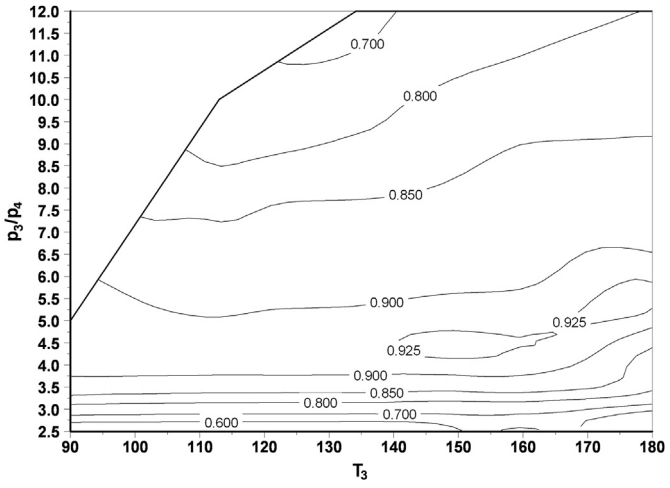

Fig. 7. Isentropic efficiency of the expansion device.

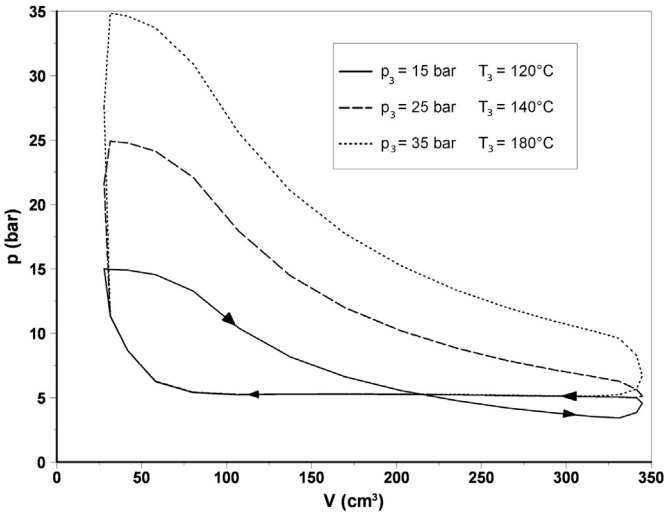

Fig. 8. Expansion device simulated cycle on the $p - V$ thermodynamic plane.

In these conditions the expansion was almost complete (Fig. 8, dashed line). Lower pressure ratios led to over-expanded cycles (continuous line), with a loss represented by the counter-clock wise area, and higher pressure ratios obviously led to under-expanded cycles (dotted line).

The resulting isentropic efficiency was comparable and in several cases even higher than a radial turbine of the same power range [44] or than a volumetric expansion device of other type (Scroll as an example) [45–49] over the most part of the investigated working conditions.

As for the delivered power, at 3000 rpm it was included within the range 10–50 kW, which is interesting for this research (Fig. 9). Based on these considerations, the value of 0.2 was therefore retained acceptable.

3.2. Collectors concentration and tilt angle

As well recognized, a high concentration improves the direct irradiation captating efficiency at high temperature, however the employment of a low concentration also implies the capability of captating more diffuse radiation and enables the plant to operate

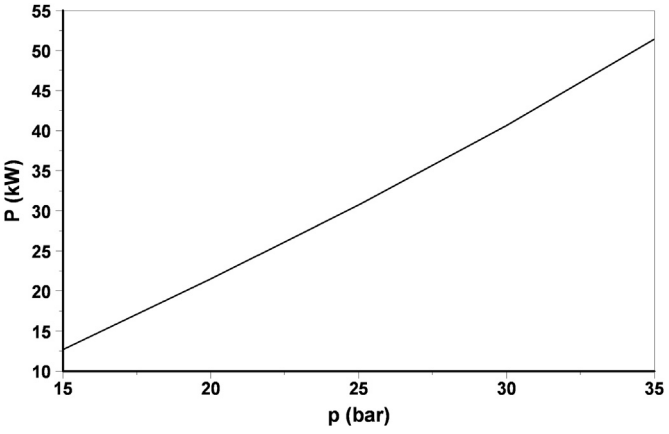

Fig. 9. Power delivered by the expansion device as a function of the inlet pressure.

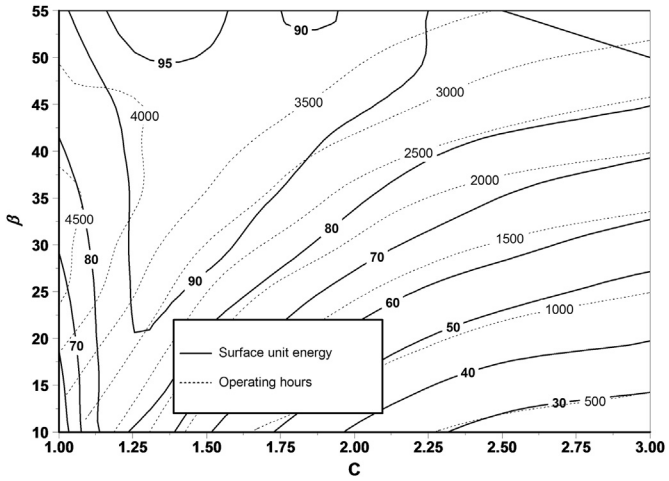

Fig. 10. Energy generated per panel unit surface (kWh/m^2) with $p_3 = 25$ bar and $T_3 = 140^\circ$C, tube model D.

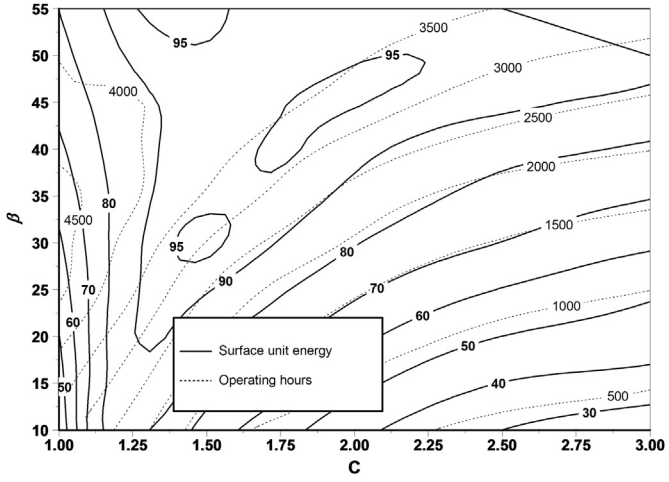

Fig. 11. Energy generated per panel unit surface (kWh/m^2) with $p_3 = 35$ bar and $T_3 = 180^\circ$C, tube model D.

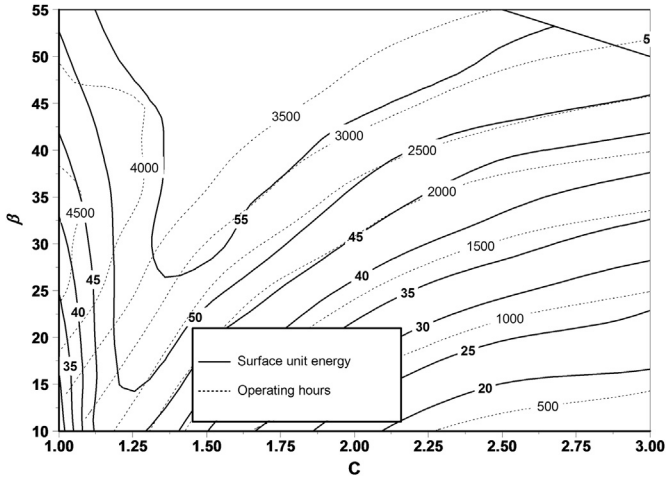

Fig. 12. Energy generated per panel unit surface (kWh/m^2) with $p_3 = 15$ bar, saturated conditions and using the tube model A.

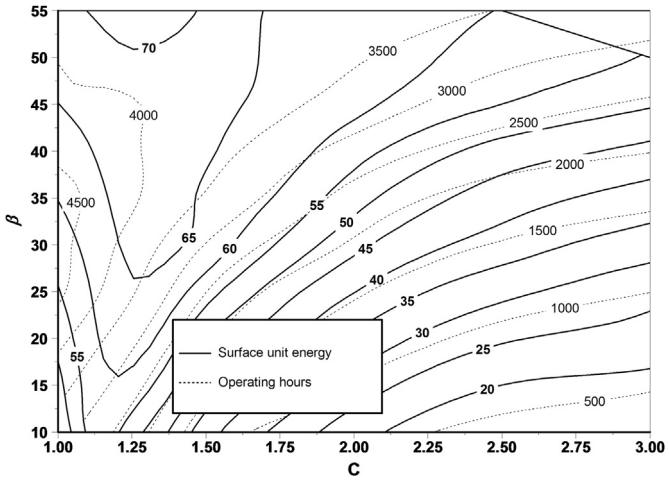

Fig. 13. Energy generated per panel unit surface (kWh/m^2) with $p_3 = 15$ bar, saturated conditions and using the tube model D.

for a larger number of hours. In the present work concentrations up to 3 were considered to avoid seasonal replacements.

The optimal annual electrical production conditions were practically the same whatever the thermodynamic parameters of the plant (Figs. 10 and 11). This trend was also found when changing the tube type, although with different values of the annual generated energy (Figs. 12 and 13). In every case, the optimal arrangements were represented by the region which is delimited at the left by C $\simeq$ 1.2 and at the right by a slanted line intersecting the first in a point whose ordinate is $\beta = 15$–20°. On the right side of the graph the annual production was nearly proportional to the number of operating hours, while on the left side it depended on the concentration.

The largest annual production per unit surface of panel was yielded when the tilt angle of the collectors is larger than 20–25°. However when the tilt angle is further increased, as widely recognized, the employed ground surface becomes larger and larger. The choice of the optimal tilt angle is therefore a tradeoff between annual energy income per unit surface of panel and ground occupation.

Tilt angle and concentration also affected the plant average specific (per panel unit surface) power even when the annual generated energy was the same, because the number of operating

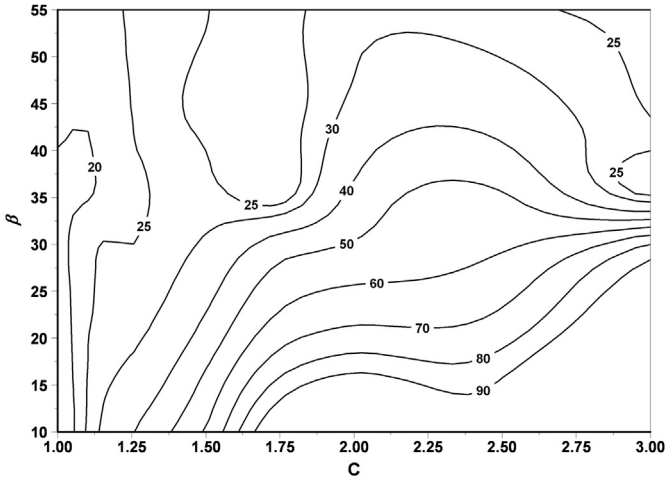

Fig. 14. Average power specific per panel unit surface (W), tube model D.

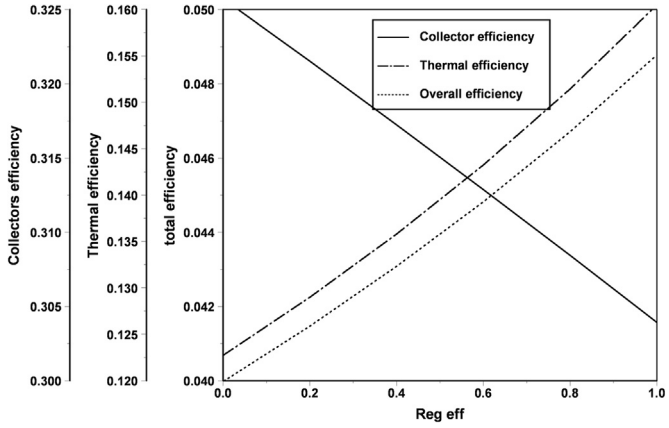

Fig. 15. Efficiency as a function of the recuperator efficiency, with $p_3 = 15$ bar and $T_3 = 160^{\circ}$C, tube model D.

hours was different (Fig. 14). Therefore it was possible to reduce the average delivered power without reducing the generated energy, with significant implications on the size of the components and hence on the initial investment costs.

3.3. Thermal cycle layout

The employment of saturated or superheated cycles was deeply studied in the literature. Some authors [50] expressed some doubts about superheating a dry fluid, but they did not take into account the regeneration of the residual heat at the outlet of the expansion device. Moreover the use of regeneration enables the partial recovery of the energy loss due to the under-expansion of the working fluid which is typical of volumetric machines.

As expected, the increase of recuperated heat produced different effects on the thermal cycle and solar field efficiency (positive effect on the first and negative on the second), since the heat transfer fluid entered the solar field at a higher temperature (Fig. 15). The simulations proved that the first effect was prevailing on the second and the overall efficiency was increased even in the less favorable conditions (winter season). In addition, a lower energetical consumption was required by the blowers since the regeneration of a part of the residual sensible heat at the end of the expansion reduced the condenser thermal load.

In order to compare saturated and superheated cycles, the results were related to the collectors efficiency degradation with temperature: although the collector model "A" had the highest optical efficiency (Fig. 7), the annual production yield was lower than collector "D", even at a very low saturation pressure and without superheating. The second model not only allowed the global efficiency (solar + thermal) to be higher, but also made convenient the use of superheating (Figs. 16 and 17). For these two tube models, the optimal conditions respectively were $p_3 = 20$ bar and saturated conditions and $p_3 = 30$ bar and $T_3 = 160\ ^{\circ}$C.

4. Conclusions

This paper summarizes the results of a research carried out to evaluate the optimal average operating conditions for a small-size solar power plant that employs stationary Compound Parabolic Collectors and a volumetric rotary expansion machine.

The proposed Wankel expansion machine allowed the use of the most suited introduction grade by means of a proper choice of the intake valves timing choice. This feature allowed to keep the isentropic efficiency equal or higher than 0.8 over the majority of the assumed working conditions and namely when the expansion ratio was within the range 3–8.

The features of the solar tubes played a fundamental role in determining the annual energy yield, since the collectors efficiency decrease rate with the temperature not only affected the amount of energy collected, but also changed the optimal thermal cycle features (saturated or superheated) and operating conditions (saturation pressure and eventual superheating temperature). The best performance was attained with $p_{sat} \simeq 30$ bar and $T_{sh} \simeq 160\ ^{\circ}$C and employing the tube model D, which showed the highest insulation properties amongst the investigated commercial types. Based on the comparison between some commercial models, in facts the annual energy production was more affected by the insulation properties than by optical efficiency, which appeared to play a secondary role when temperatures above 80–90 °C were needed.

As for the solar field optimal parameters, the best performance was yielded with a concentration ensuring at least 3000 operating hours per year: the energy production was maximized when concentration was in the range 1.1–1.4, which in fact allowed the plant to be operated for 3000–3500 h per year. Although an amount of energy close to the maximum may be collected with different

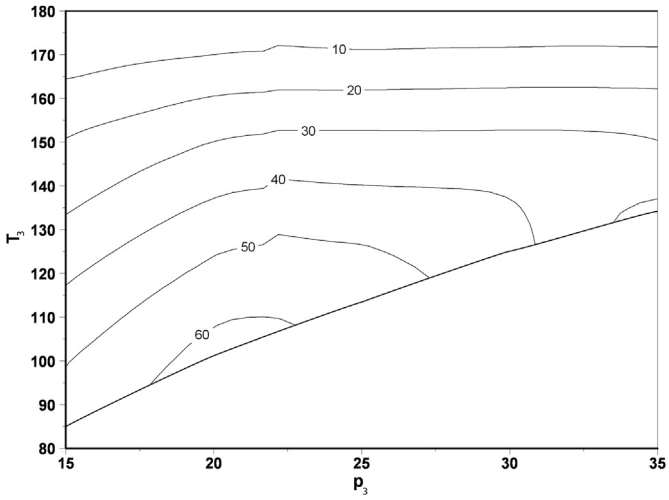

Fig. 16. Energy generated per panel unit surface (kWh/m^2) using the tube model A with $C = 1.25$ and $\beta = 25^{\circ}$.

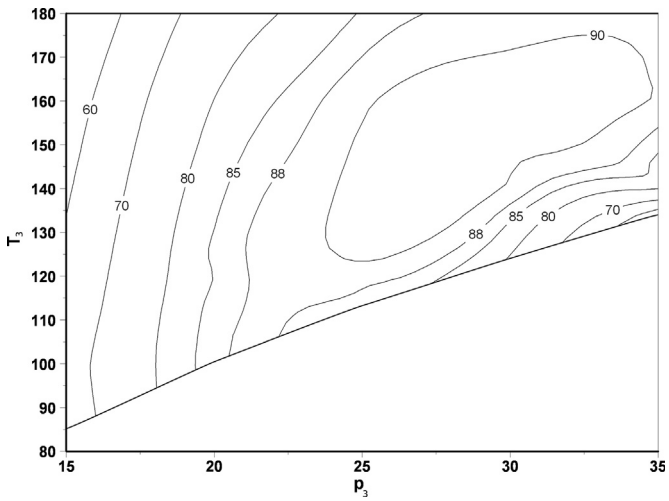

Fig. 17. Energy generated per panel unit surface (kWh/m^2) using the tube model D with $C = 1.25$ and $\beta = 25^{\circ}$.

combinations of C and β, a reasonable tradeoff between energy yield per collectors' unit surface and occupied ground surface may be achieved by using a tilt angle smaller than 20–25°.

The importance of C and β was not limited only to the amount of generated energy. A proper choice of these two parameters maximized the number of operating hours without an appreciable reduction of the energy specific production. This feature enables the reduction of the initial investment cost because the size of the various components (heat exchangers, pumps, aerocondensers and relative blowers, connection pipes) can be decreased.

References

[1] Duffie JA, Beckman WA. Solar thermal engineering. Madison: John Wiley and Sons; 1980.
[2] Pei Gang, Li Jing, Ji Jie. Analysis of low temperature solar thermal electric generation using regenerative organic Rankine cycle. Appl Therm Eng 2010;30(89):998–1004.
[3] Jing L, Gang P, Ji Jie. Optimization of low temperature solar thermal electric generation with organic Rankine cycle in different areas. Appl Energy 2010;87(11):3355–65.
[4] Amoresano A, Langella G, Meo S. Cycle efficiency optimization for ORC solar plants. Int Rev Mech Eng 2013;7(5):888–94.
[5] Davidson TA. Design and analysis of a 1 kW Rankine power cycle, employing a multi-vane expander, for use with a low temperature solar collector. Bachelor Thesis. MIT; 1977.
[6] Badr O, Probert SD, OCallaghan P. Performances of multivane expanders. Appl Energy 1985;20:207–34.
[7] Wang XD, Zhao L, Wang JL, Zhang WZ, Zhao XZ, Wu W. Performance evaluation of a low-temperature solar Rankine cycle system utilizing R245fa. Sol Energy 2010;84:353–64.
[8] Wolpert JL, Riffat SB. Solar-powered Rankine system for domestic applications. Appl Therm Eng 1996;16:281–9.
[9] McMahan A. Design and optimization of organic Rankine cycle solar thermal powerplants. MSc. Thesis. Madison: University of Wisconsin; 2006.
[10] Delgado-Torres AM, Garcia-Rodriguez L. Comparison of solar technologies for driving a desalination system by means of an organic Rankine cycle. Desalination 2007;216:276–91.
[11] Delgado-Torres AM, Garcia-Rodriguez L. Analysis and optimization of the low-temperature solar organic Rankine cycle (ORC). Energy Convers Manag 2010;51:2846–56.
[12] Bruno JC, Lopez-Villada J, Letelier E, Romera S, Coronas A. Modelling and optimisation of solar organic rankine cycle engines for reverse osmosis desalination. Appl Therm Eng 2008;28:2212–26.
[13] Wang JL, Zhao L, Wang XD. A comparative study of pure and zeotropic mixtures in low-temperature solar Rankine cycle. Appl Energy 2010;87:3366–73.
[14] Kane M, Larrain D, Favrat D, Allani Y. Small hybrid solar power system. Energy 2003;28:1427–43.
[15] Prabhu E, National Renewable Energy Laboratory (US). Solar trough organic Rankine electricity system (STORES). Stage 1. power plant optimization and economics November 2000–May 2005. Golden, Colo: National Renewable Energy Laboratory; 2006.
[16] Canada S, Cohen G, Cable R, Brosseau D, Price H. Parabolic trough organic Rankine cycle solar power plant. Denver, Colorado: DOE Solar Energy Technologies; 2004.
[17] Manolakos D, Papadakis G, Kyritsis S, Bouzianas K. Experimental evaluation of an autonomous low-temperature solar Rankine cycle system for reverse osmosis desalination. Desalination 2007;203:366–74.
[18] Winston R. Principles of solar concentrators of a novel design. Sol Energy 1974;16(2):89–95.
[19] Winston R, Hinterberger H. Principles of cylindrical concentrators for solar energy. Sol Energy 1975;17(4):255–8. Macmillan; 1979.
[20] Rabl A. Comparison of solar concentrators. Sol Energy 1976;18(2):93–111.
[21] Rabl A. Solar concentrators with maximal concentration for cylindrical absorbers. Appl Opt 1976;15(7):1871–3.
[22] Buttinger F, Beikircher T, Pröll M, Schölkopf W. Development of a new flat stationary evacuated CPC-collector for process heat applications. Sol Energy 2010;84(7):1166–74.
[23] Mills DR, Bassett IM, Derrick GH. Relative cost-effectiveness of CPC reflector designs suitable for evacuated absorber tube solar collectors. Sol Energy 1986;36(3):199–206.
[24] Vargas JVC, Ordonez JC, Dilay E, Parise JAR. Modeling, simulation and optimization of a solar collector driven water heating and absorption cooling plant. Sol Energy 2009;83(8):1232–44.
[25] Probert SDHM, OCallaghan PW, Bala E. Design optimisation of a solar-energy harnessing system for stimulating an irrigation pump. Appl Energy 1983;15.
[26] Monahan J. Development of a 1-kW, organic Rankine cycle power plant for remote applications. New York: Intersociety Energy Conversion Engineering Conference; 1976.
[27] Wang J, Yan Z, Zhao P, Dai Y. Off-design performance analysis of a solar-powered organic Rankine cycle. Energy Convers Manag 2014;80:150–7.
[28] Antonelli M, Baccioli A, Francesconi M, Lensi R, Martorano L. Analysis of a low concentration solar plant with compound parabolic collectors and a rotary expander for electricity generation. Energy Procedia 2013;45:170–9.
[29] Quoilin S, Orosz M, Hemond H, Lemort V. Performance and design optimization of a low-cost solar organic Rankine cycle for remote power generation. Sol Energy 2011;85(5):955–66.
[30] Badr O, Naik S, O'Callaghan PW, Probert SD. Rotary Wankel engines as expansion devices in steam Rankine-cycle engines. Appl Energy 1991;39(1):59–76.
[31] Badr O, Naik S, O'Callaghan PW, Probert SD. Wankel engines as steam expanders: design considerations. Appl Energy 1991;40(2):157–70.
[32] Antonelli M, Martorano L. A study on the rotary steam engine for distributed generation in small size power plants. Appl Energy 2012;97:642–7.
[33] Antonelli M, Baccioli A, Francesconi M, Desideri U, Martorano L. Operating maps of a rotary engine used as an expander for micro-generation with various working fluids. Appl Energy 2014;113:742–50.
[34] Liu BYH, Jordan RC. The inter-relationship and characteristic distribution of direct, diffuse and total solar radiation. Sol Energy 1960;4(3):119.
[35] Thermal solar system and components – solar collectors test methods. 2006. EN 12975–2 European Standards.
[36] Zambolin E, del Col D. An improved procedure for the experimental characterization of optical efficiency in evacuated tube solar collectors. Renew Energy 2012;43:37–46.
[37] Zhang W, Ma X, Omer SA, Riffat SB. Optimum selection of solar collectors for a solar-driven ejector air conditioning system by experimental and simulation study. Energy Convers Manag 2012;63:106–11.
[38] Zhang XR, Yamaguchi H. An experimental study on evacuated tube solar collector using supercritical CO_2. Appl Therm Eng 2008;28(10):1225–33.
[39] Ma L, Lu Z, Zhang J, Liang R. Thermal performance analysis of the glass evacuated tube solar collector with U-tube. Build Environ 2010;45(9):1959–67.
[40] Atkins MJ, Walmsley MRW, Morrison AS. Integration of solar thermal for improved energy efficiency in low-temperature-pinch industrial processes. Energy 2010;35(5):1867–73.
[41] Antonelli M, Baccioli A, Francesconi M, Martorano L. Experimental and numerical analysis of the valve timing effects on the performances of a small volumetric rotary expansion device. Energy Procedia 2013;45:1077–86.
[42] Badami M, Mura M. Preliminary design and controlling strategies of a small-scale wood waste Rankine cycle (RC) with a reciprocating steam engine (SE). Energy 2009;34(9):1315–24.
[43] Quoilin S, Lemort V. In: Technological and economical survey of organic Rankine cycle systems. Fifth european conference economics and management of energy in industry, Algarve, Portugal; 14–17 April 2009.
[44] Fiaschi D, Manfrida G, Maraschiello F. Thermo-fluid dynamics preliminary design of turbo-expanders for ORC cycles. Appl Energy 2012;97:601–8.
[45] Lemort V, Quoilin S, Cuevas C, Lebrun J. Testing and modeling a scroll expander integrated into an organic Rankine cycle. Appl Therm Eng 2009;29(14–15):3094–102.
[46] Declaye S, Quoilin S, Guillaume L, Lemort V. Experimental study on an open-drive scroll expander integrated into an ORC (organic Rankine cycle) system with R245fa as working fluid. Energy 2013;55:173–83.
[47] Quoilin S, Lemort V, Lebrun J. Experimental study and modeling of an organic Rankine cycle using scroll expander. Appl Energy 2010;87(4):1260–8.
[48] Guangbin L, Yuanyang Z, Liansheng L, Pengcheng S. Simulation and experiment research on wide ranging working process of scroll expander driven by compressed air. Appl Therm Eng 2010;30(14–15):2073–9.
[49] Clemente S, Micheli D, Reini M, Taccani R. Energy efficiency analysis of organic Rankine cycles with scroll expanders for cogenerative applications. Appl Energy 2012;97:792–801.
[50] Chen H, Goswami DY, Stefanakos EK. A review of thermodynamic cycles and working fluids for the conversion of low-grade heat. Renew Sustain Energy Rev 2010;14(9):3059–67.